Heterozygous missense mutations in *NFATC1* are associated with atrioventricular septal defect

Rosangela Ferese,[1] Monica Bonetti,[2] Federica Consoli,[3] Valentina Guida,[3] Anna Sarkozy,[3] Francesca R. Lepri,[4] Paolo Versacci,[5] Stefano Gambardella,[1] Giulio Calcagni,[4] Katia Margiotti,[3] Francesca Piceci Sparascio,[3] Hossein Hozhabri,[3,6] Tommaso Mazza,[7] Maria Cristina Digilio,[4] Bruno Dallapiccola,[4] Marco Tartaglia,[4] Bruno Marino,[5] Jeroen den Hertog,[2,8,*] Alessandro De Luca[3,*]

[1]IRCCS Neuromed, Localita` Camerelle, 86077 Pozzilli (IS), Italy; [2]Hubrecht Institute-KNAW and University Medical Center Utrecht, 3584CT Utrecht, The Netherlands; [3]Molecular Genetics Unit, Casa Sollievo della Sofferenza Hospital, IRCCS, 71013 San Giovanni Rotondo, Italy; [4]Bambino Gesù Children Hospital, IRCCS, 00146 Rome, Italy; [5]Division of Pediatric Cardiology, Department of Pediatrics, "Sapienza" University, 00161 Rome, Italy; [6]Department of Experimental Medicine, Sapienza University of Rome, 00161 Rome, Italy; [7] Bioinformatics Unit, Casa Sollievo della Sofferenza Hospital, IRCCS, 71013 San Giovanni Rotondo, Italy; [8]Institute of Biology, 2300RC Leiden, The Netherlands.

*These authors equally contributed as senior authors in this work.

This article has been accepted for publication and undergone full peer review but has not been through the copyediting, typesetting, pagination and proofreading process, which may lead to differences between this version and the Version of Record. Please cite this article as doi: 10.1002/humu.23593.

Correspondence to:

Alessandro De Luca, PhD,

Istituto CSS-Mendel, Viale Regina Margherita 261, 00198 Rome, Italy,

Tel.: +39 06 44160510, Fax: +39 06 44160548, E-mail: a.deluca@css-mendel.it

Grant Sponsor: Italian Ministry of Health RF 2010 2310935 and RC 2016 to ADL, the Research Council for Earth and Life Sciences [ALW 819.02.021] with financial aid from the Netherlands Organisation for Scientific Research (NWO) (to J.d.H.), and Fondazione Bambino Gesù (CUoRE) to MT.

ABSTRACT (197 words)

Atrioventricular septal defect (AVSD) may occur as part of a complex disorder (*e.g.*, Down syndrome, heterotaxy), or as isolate cardiac defect. Multiple lines of evidence support a role of calcineurin/NFAT signaling in AVSD, and mutations in *CRELD1*, a protein functioning as a regulator of calcineurin/NFAT signaling have been reported in a small fraction of affected subjects.

In this study, 22 patients with isolated AVSD and 38 with AVSD and heterotaxy were screened for *NFATC1* gene mutations. Sequence analysis identified three missense variants in three individuals, including a subject with isolated AVSD [p.(Ala367Val)], an individual with AVSD and heterotaxy [p.(Val210Met)] and a subject with AVSD, heterotaxy and oculo-auriculo-vertebral spectrum (OAVS) [p.(Ala696Thr)], respectively. The latter was also heterozygous for a missense change in *TBX1* [p.(Pro86Leu)]. Targeted resequencing of genes associated with AVSD, heterotaxy or OAVS excluded additional hits in the first two subjects. Functional characterization of NFATC1 mutants documented defective nuclear translocation

and decreased transcriptional transactivation activity. When expressed in zebrafish, the three NFATC1 mutants caused cardiac looping defects and altered atrioventricular canal patterning, providing evidence of their functional relevance *in vivo*.

Our findings support a role of defective *NFATC1* function in the etiology of isolated and heterotaxy-related AVSD.

Key words: Congenital heart defect, atrioventricular septal defect, heterotaxy, oculo-auriculo-vertebral spectrum, *NFATC1*.

INTRODUCTION

Congenital heart defects (CHDs) are the most common birth defects worldwide, occurring in 4-8/1,000 live births [Ferencz *et al*. 1985]. In a significant fraction of cases, CHDs are caused by chromosomal anomalies or gene mutations, manifesting either as isolated disorder or as an associated defect in the context of a multisystem disease. CHDs with an established genetic cause account for less than 20% of cases, and the underlying molecular cause of the majority of isolated CHDs still remains uncharacterized.

Atrioventricular septal defect (AVSD; MIM# 606215) comprises a series of different anomalies of the atrioventricular valves, and atrial and ventricular septa. They represent up to 7% of all CHDs, and their prevalence ranges from 0.3 to 0.4 per 1,000 live births [Calkoen *et al*., 2016; Reller *et al.* 2008]. Based on large fetal echocardiographic series, AVSD prevalence has been estimated to be much higher in utero, accounting for 18% of CHD affected fetuses. AVSD can be either complete or partial. The former represents approximately 70% of total AVSD cases, and in general consists of a single common atrioventricular valve and an atrial septal defect (ostium primum) confluent with a posterior ventricular septal defect in the inlet portion of the ventricular septum. In the partial form, including the remaining 30% of cases, two separate right and left atrioventricular valves (with a cleft of the anterior leflet of the mitral valve) and an atrial septal defect (ostium primum), in absence of ventricular septal communication, are commonly observed. Isolated cleft of the mitral valve is considered a less severe form of AVSD [DiSegni *et al.* 1985]. In families of patients with AVSD, recurrence of CHD in siblings has been reported in 3–4% of cases [Digilio *et al.* 1993], supporting to a multifactorial model of inheritance. In a subset of families, however, recurrent CHD is prevalently concordant and transmission of the disease

fits with an autosomal dominant model, with monogenic or oligogenic inheritance [Digilio *et al.* 1993].

Large studies estimate that more than two thirds of infants with AVSD display a cytogenetic abnormality, with trisomy 21 being the most common. In a unselected series of more than 600 patients, Down syndrome (DS; MIM# 190685) and heterotaxy syndrome (HTX; MIM# 606217) accounted for about 45% and 15% of AVSD cases, with other genetic or syndromic disorders representing an additional 15% [Digilio *et al.* 1999]. In the same series, isolated AVSD accounted for 25% of affected individuals [Digilio *et al*. 1999]. In addition to DS and HTX, other disorders having AVSD as associated feature include Ellis-van Creveld syndrome (MIM# 225500), Oro-Facio-Digital syndrome II (MIM# 252100), Kaufman-McKusick syndrome (MIM# 236700), Smith-Lemli-Opitz syndrome (MIM# 270400), CHARGE syndrome (MIM# 214800), and Noonan syndrome (MIM# 163950) [Digilio *et al*. 1999; 2018]. AVSD typically occurs in patients with 8p23 and 3p25-26 deletion syndromes [Giglio *et al*. 2000; Green *et al*. 2000]. Deletion 8p23 encompasses *GATA4* gene, which encodes for a transcription factor with important role in cardiac development, whose missense mutations have been reported in selected families with isolated AVSD [Garg *et al*. 2003]. Deletion 3p25-26 comprises *CRELD1*, the first gene to be associated with AVSD [Robinson *et al*. 2003]. An additional locus for isolated AVSD has been mapped to chromosome 1p31-p21 [Sheffield *et al.* 1997], but the relevant disease gene still remains unknown. Moreover, dominant negative-acting mutations in the transforming growth factor-beta receptor *ALK2* have also been reported in AVSDs [Smith *et al*. 2009]. Recently, application of next generation sequencing (NGS) to explore the molecular causes of AVSDs has allowed to identify rare causal variants in *NR2F2* [Al Turki *et al*. 2014] and other genes with biological relevance to AVSD (e.g., *NIPBL*, *CHD7*, *CEP152*, *BMPR1a*, *ZFPM2*, and *MDM4*)

[D'Alessandro *et al.* 2016]. Among these, mutations in *NIPBL*, *CHD7*, and *CEP152* have also been implicated in developmental disorders, further emphasizing their pleiotropic effect on development.

NFATC1 is a member of the Rel/NF-kB family of transcription factors that were first reported as key regulators of T-cell activation. Five proteins of this family (NFATC1–5) are found in mammals, all playing non-redundant roles during embryonic and postnatal development [Wu *et al.* 2013]. NFATs regulate proliferation, differentiation, and homeostasis in numerous cell types during embryogenesis and throughout life [Crabtree GR, 1999]. *NFATC1* is required for cardiac development. Mice homozygous for a disrupted *Nfatc1* gene do not develop normal cardiac valves and septa, and die of circulatory failure during embryonic development [de la Pompa *et al.* 1998; Ranger *et al.* 1998]. *NFATC1* gene mutations have not been linked to human diseases so far, but missense mutations in *CRELD1*, an important regulator of the calcineurin/NFATC1 signaling, were found to occur in approximately 5–10% of individuals with AVSD, including isolated AVSD [Guo *et al*. 2010; Posch *et al*. 2008; Robinson *et al.* 2003; Zatyka *et al*. 2005], AVSD in individuals with Down syndrome [Asim *et al*. 2018; Guo *et al*. 2010; Maslen *et al.* 2006], and AVSD in the context of HTX [Robinson *et al.* 2003; Zhian *et al*. 2012]. These data argue that defective NFATC1 function could contribute to AVSD, and prompted the search of *NFATC1* mutations in two cohorts of patients, including both isolated AVSD and AVSD associated with HTX. We report the identification of *NFATC1* rare variants in a small but significant proportion of cases of both cohorts. Using immunofluorescence and luciferase assays, we provide *in vitro* data documentation for defective/impaired function of the disease-associated mutants. Finally, we showed that expression of each of the NFATC1 mutants cause heart defects in zebrafish embryos. Taken

together, these data provide evidence for the requirement of proper NFATC1 function in cardiac development.

Methods

Study cohort

The study cohort included 60 unrelated individuals with AVSD (30 males and 30 females) comprising 22 patients with non-syndromic AVSD and 38 with AVSD in the context of HTX. Complete and partial AVSD were equally represented. Supp. Table S1 shows the demographic and clinical characteristics for each patient. Cardiovascular diagnosis was obtained by echocardiography in all cases. Standard cytogenetic and 22q11 deletion analyses were performed on all subjects as previously described [Amati *et al.* 1995], excluding the presence of any chromosomal rearrangements and anauploidies. All study participants had previously been tested for *CRELD1*, *GATA4, PTPN11* and *NR2F2* mutations by either denaturing high-performance liquid chromatography (DHPLC) and/or direct DNA sequencing, excluding occurrence of causative mutations in these genes (Sarkozy *et al.* 2005, 2006; De Luca A. unpublished data). DNA samples from 870 unrelated and healthy population-matched individuals served as controls. Of these, 70 subjects were sequenced for the entire coding region of the *NFATC1* gene (NM_006162.4) and its exon-intron junctions to examine the genetic variabily of this gene in a group of ethnically matching healthy individuals. Informed consents were obtained from parents or guardians of both patients and controls. Research protocols and procedures were approved by the Institutional Review Board of the participating institutes.

NFATC1 Mutational Analysis

Genomic DNA was extracted from peripheral blood with standard protocols. The coding exons and intronic stretches flanking the splice sites of the *NFATC1* gene were scanned by DHPLC and direct DNA sequencing. Primers, and PCR and DHPLC conditions are available on request. Numbering for all the variants started at the adenine nucleotide (A) in the ATG initiation codon. For protein sequences, the codon for the initiator methionine was codon 1. The NCBI HomoloGene tool (http://www.ncbi.nlm.nih.gov/homologene) was used to analyze the level of conservation of sequence variants in orthologous genes. The functional impact of the identified amino acid substitutions was assessed *in silico* using the Combined Annotation Dependent Depletion (CADD) tool [Kircher et al. 2014], which scores the deleteriousness of variants by integrating multiple functional categories into one metric. Based on this metric, the bottom 90% of all single nucleotide varints (~8.6 billion, GRCh37/hg19) are compressed into (phred-like) scaled CADD units < 10, while the top 10% to 1% (~774 million variants) display CADD scores between 10 and 20. Finally, a score ≥20 indicates the 1% most deleterious variants. To apply a cutoff on deleteriousness, CADD values above 15 were classified as deleterious [Kircher et al. 2014].

Next Generation Sequencing

An opportunely designed custom TruSight One sequencing panel kit (Illumina, San Diego, CA, USA) was used to analyze a panel of 38 selected OMIM genes, including 20 genes related to HTX, 14 genes associated to ASVD and 4 genes related to OAVS (Supp. Table S2). The enriched libraries were sequenced by a NextSeq 500 instrument (Illumina, San Diego, CA, USA). NGS data analysis was performed using an in-house implemented pipeline. In particular, we considered only novel or rare variants with a minor allele frequency <1% in databases (dbSNP, GO-ESP and ExAC). The candidate variant selection was carried out taking into account the available clinical data of the affected individual.

Plasmid Construction of NFATC1 Expression Vectors

For fluorescent microscopy analyses, full-length human *NFATC1* was subcloned into the pEGFP–N1 (kindly provided by Prof. Martin F. Schneider, University of Maryland School of Medicine, Baltimore, MD, USA), to introduce an enhanced green fluorescence protein (EGFP) tag at the C-terminus. *NFATC1* variants [p.(Val210Met), p.(Ala367Val) and p.(Ala696Thr)] were introduced by site-directed mutagenesis (QuikChange II XL, Stratagene, La Jolla, CA, USA). A nuclear localization signal (NLS; ProLysLysLysArgLysVal) was introduced in the *NFATC1-EGFP* construct (*Bam*HI) to promote efficient nuclear translocation of ectopically expressed proteins. For transactivation assays, the *NPPB* promoter (-36320 to -34624, hg19), which contains binding sites for NFAT proteins [Molkentin *et al.* 1998], was cloned upstream of the luciferase gene (*Xho*I-*Hind*III sites) of the pGL2 reporter plasmid (pGL2-NPPB-Luc). For *in vivo* studies, human *NFATC1* was cloned (*Cla*I/*Xba*I sites) in the pCS2+ expression vector (pCS2+-*NFATC1*). All constructs were verified by sequencing.

Immunofluorescence studies

For immunofluorescent staining, COS-7 cells were transfected with wild-type *NFATC1*-pEGFP-N1 or each of the three mutants, p.(Val210Met), p.(Ala367Val), and p.(Ala696Thr), using lipofectamine 2000 (Invitrogen Life Technologies, Carlsbad, CA, USA), as indicated by the manufacturer protocol. In co-transfection experiments, COS-7 cells were transfected with equal amounts of the wild-type *NFATC1*-pEGFP-N1 expressing plasmid in combination with each of the three mutant constructs. Cells were fixed after 48h with 4% paraformaldehyde, permeabilized with 0.5% Triton X-100, and stained with red-fluorescent Alexa Fluor-568 phalloidin antibody (Molecular Probes, Eugene, OR, USA) for actin cytoskeleton detection. The extensively rinsed cover glass was then mounted on the microscope slide using Vectashield Mounting Medium with DAPI (Vector Laboratories, Burlingame, CA). Imaging was performed on a Leica CTS SP1 AOBS confocal microscope (Leica Microsystems, Mannheim, Germany).

Luciferase reporter gene assays

COS-7 cells were manteined in Dulbecco's modified Eagle's medium containing 10% fetal calf serum (Life Technologies, Grand Island, NY, USA). Cells at approximately 90% confluence were transfected with plasmids using lipofectamine2000 reagent (Invitrogen Life Technologies, Carlsbad, CA, USA). As an internal control, pRL-TK, which expresses the Renilla luciferase, was used to normalize transfection efficiency. 250 ng of wild-type or mutant *NFATC1* construct was cotrasfected with 50 ng of pGL2-NPPB-Luc reporter and 5 ng of pRL-TK control vector. To simulate heterozygosity of the mutations, cells were co-transfected with an equal amount of wild-type and each of the mutant *NFATC1* expression

vectors. Cells were harvested and lysed 48h after transfection, and then the Firefly and Renilla luciferase activities were measured with the Dual-Glo luciferase assay system (Promega, Madison, WI, USA). All transfection experiments were conducted in triplicates and repeated at least three times independently. The activity of the *NPPB* promoter was presented as fold activation of Firefly luciferase relative to Renilla luciferase.

Cytoplasmic and nuclear extractions

To induce the protein to translocate into the nucleus, COS-7 cells transfected with wild-type or each of the *NFATC1* mutants were treated with 3 μM ionomycin (Sigma Aldrich St. Louis, MO, USA) for 30 minutes, 24 hours after transfection. Following transfection of the wild-type or mutant *NFATC1*-pEGFP-N1 construct and treatment with ionomycin, $20x10^6$ COS-7 cells were resuspended in buffer A (10 mM Hepes or Tris-HCl [pH 7.5], 40 mM KCl, 2 mM $MgCl_2$, 10% glycerol, 1 mM NaPPi, 1μg/mL pepstatin, 1μg/mL aprotinin, 1μg/mL leupeptin, 1mM NaVO4, 1 mM NaF, 1 mM PMSF), incubated on ice for 30 minutes, and centrifuged for 5 minutes. Cytoplasmic extracts were saved. Nuclear pellets were cleaned with 25 M sucrose buffer (25 M sucrose, 1 M $MgCl_2$, 1M HEPES [pH 7.4]) and 35 M sucrose buffer (35 M sucrose, 1 M $MgCl_2$, 1 M HEPES [pH 7.4]). Then, pellets were resuspended in buffer B (10 mM Hepes or Tris-HCl [pH 7.5], 500mM NaCl, 1% Triton-X100, 10% glycerol, 1 mM NaPPi, 1 μg/mL pepstatin, 1 μg/mL aprotinin, 1 μg/mL leupeptin, 1 mM NaVO4, 1 mM NaF, 1 mM PMSF), sonicated for 1 minute, centrifuged and saved.

Western blotting

Immunoblotting was carried out using standard methodologies. For NFATC1 protein detection, rabbit monoclonal anti-EGFP antibody (Cell Signaling Technology, New England

Biolabs Biolabs, Hertfordshire, UK) was used as primary antibody. Mouse anti-GM130 monoclonal antibody (cis-Golgi Marker) (Abcam Inc., Cambridge, MA, USA) was used as a control for the cytoplasmic extract, and rabbit monoclonal anti-H3 (Histone H3) antibody (Abcam Inc., Cambridge, MA, USA) was used as a control for proper nuclear extract. Secondary antibodies specific to mouse or rabbit were purchased from BD Bioscience Pharmaceutical (Franklin Lakes, NJ, USA). Blots were visualized by the enhanced chemiluminescence system (ECL Western Blotting Detection Kit, GE Healthcare Life Sciences, Little Chalfont, UK). Western blots were repeated a minimum of 3 times to confirm reproducibility. Densitometric analysis was performed using ImageJ software. Data were repeated a minimum of 3 times to confirm reproducibility.

Zebrafish embryo injections and in situ hybridization and histological analysis

Zebrafish were kept, and the embryos were staged as described previously [Westerfield, 1993]. All procedures involving experimental animals were approved by the local animal experiments committee and performed in compliance with local animal welfare laws, guidelines and policies, according to national and European law. Wild-type and mutated [p.(Val210Met), p.(Ala367Val), and p.(Ala696Thr)] *NFATC1* pCS2+- constructs were linearized with *Not*I enzyme and capped mRNA prepared with the Message Machine kit (Ambion, Austin, TX, USA). mRNA injections were performed at the one-cell stage. Morphological phenotypes were assessed at 24 hours and 48 hours postfertilization (hpf). To investigate cardiac defects, embryos were anesthetized at 48 hpf with MS-222 (Sigma Aldrich St. Louis, MO, USA), and fixed in 4% paraformaldehyde. *In situ* hybridizations were carried out as described previously [Thisse *et al.* 1993], using probes specific for the following heart proteins: cardiac myosin light chain 2 (*myl7*), atrial myosin heavy chain

(*amhc*) (also known as *myh6*), ventricular myosin heavy chain (*vmhc*), atrial natriuretic factor (*anf*), bone morphogenetic protein 4 (*bmp4*), T-box transcription factor 2b (*tbx2b*), nuclear factor of activated T cells (*nfat*), and hyaluronan synthase 2 (*has2*). Embryos were cleared in methanol and mounted in 100% glycerol before pictures were taken. Phenylthiourea was added to suppress pigmentation in developing embryos at 48 hpf. To evaluate AVC formation, histological analysis of the heart were conducted on six injected embryos for the wild-type and each of the three mutants. Zebrafish embryos were mounted in Technovit 8100 (Kulzer, Wehrheim, Germany), and sections of 7 μm thickness were cut with a microtome (Reichert-Jung 2050, Leica Microsystems, Wetzlar, Germany). Counterstaining was done using 0.05% neutral red, staining all nuclei. Sections were mounted in Pertex.

Statistical analyses

Statistical analyses were performed using GraphPad Prism Software, version 5.0. Data were expressed as means ± SD, unless otherwise indicated. Continuous variables were tested for normal distribution and one-way ANOVA was used for the comparison of numeric variables between groups. Fisher's exact test was used to compare the number of individuals with rare (minor allele frequency < 1%) *NFATC1* variants between AVSD cases and controls. Student's t-test was used to establish statistical significance in luciferase experiments. A P value < 0.05 indicated significant differences.

Results

NFATC1 mutation screening

Sixty individuals with AVSD, including 22 subjects with non-syndromic AVSD and 38 with AVSD in the context of HTX, were screened for *NFATC1* mutations by DHPLC analysis

followed by confirmatory sequencing of positive DHPLC patterns. Seventy population-matched unaffected subjects were also screened as controls. Mutation screening allowed to identify three heterozygous *NFATC1* missense variants, two of which [p.(Val210Met) and p.(Ala696Thr)] were found in the subgroup of HTX patients (2/38, ~5.2%), and one, p.(Ala367Val), in the cohort of non-syndromic AVSD cases (1/22, ~4.5%). No nonsynonymous variant was identified in the control group (Fisher's exact test, one-tailed: $p = 0.0957$). Parental DNA specimens were not available for any of the three probands. To exclude that the identified changes were variants occurring in the Italian population, additional 1,600 population-matched unaffected control chromosomes were screened for the presence of those mutants by sequence analysis, and none carried the identified changes. p.(Val210Met), which was identified in a sporadic subject with partial AVSD and HTX with polysplenia (left isomerism), alters an evolutionarily conserved amino acid residue (Supp. Figure S1) within the *N*-terminal transactivation domain A (TAD-A, residues 126 to 218) that mediates NFATC1 binding to CREBBP/ EP300, a member of a family of coactivators involved in the regulation of transcription and chromatin remodeling [Meissner *et al.* 2011; García-Rodríguez and Rao, 1998]. The change had been previously reported at very low MAF in public databases (c.628G>A, rs62096875), and was predicted to be high-impact variant (or deleterious) by CADD algorithm (scaled CADD score = 28.8). p.(Ala367Val) was found in a sporadic individual with non-syndromic partial AVSD (CA12), and affected a moderately conserved amino acid (Supp. Figure S1) located in a region functionally uncharacterized and positioned downstream of the first nuclear export signal (NES) (residues 310 to 321) and upstream of the second NLS (residues 682 to 684) of the protein. The missense change had previously been annotated in public databases (ESP6500 and ExAC) as a rare variant (c.1100C>T, rs367652299; $MAF_{ESP6500} = 7.7E\text{-}5$, $MAF_{ExAC} = 2.9E\text{-}5$) and was

predicted to be a low-impact variant (or benign) by CADD bioinformatics tool (scaled CADD score = 9.984). The third variant, p.(Ala696Thr), was found in a sporadic patient with complete AVSD and both HTX with polysplenia (left isomerism) and oculo-auriculo-vertebral-spectrum (OAVS) as extra-cardiac findings. The variant affected a highly conserved amino acid residue (Supp. Figure S1) located close to the second NLS motif (residues 682 to 684), which mediates NFATC1 nuclear translocation. p.(Ala696Thr) had not previously been reported in public databases, and was predicted to be a high-impact variant (or deleterious) by CADD (scaled CADD score = 24.5). All of these mutations have been included in the LOVD database (https://databases.lovd.nl/shared/variants/NFATC1/unique). DNA sequence chromatograms of the *NFATC1* variants, corresponding predictions from bioinformatics tools and information on allele frequency in Italian controls and public databases, and anatomical characteristics of mutation-positive patients are summarized in Figure 1A, 1B and 1C.

To verify if *NFATC1* mutation-positive patients carried genetic variations in other genes associated to AVSD, HTX or OAVS, targeted resequencing was used to test a panel of 14 genes associated to AVSD, 20 genes involved in heterotaxy, and 4 genes associated to OAVS. No potentially pathogenic variant was found in patient CA12 with non-syndromic partial AVSD and in patient HD239 with partial AVSD and HTX with polysplenia, whereas a likely pathogenic variant was detected in *TBX1* gene [NM_080647.1: c.257C>T; p.(Pro86Leu)] in patient IS18 with complete AVSD and both HTX with polysplenia (left isomerism) and oculo-auriculo-vertebral-spectrum (OAVS). This *TBX1* missense change had previously been annotated in public databases (gnomAD exomes) as a rare variant (c.257C>T, rs775295536; MAF_{gnomAD}= 8.78838E-05) and was predicted to be a high-impact variant (or deleterious) by bioinformatics tool (scaled CADD score = 21.4).

In vitro functional characterization of the AVSD-associated NFATC1 mutants

NFATC1 is a transcription factor whose activity is controlled by the Ca^{2+}/Calmodulin-dependent phosphatase, calcineurin. Inactive NFATC1 resides in the cytoplasm. In response to sustained elevated calcium levels, NFATC1 is dephosphorylated by calcineurin, which induces rapid NFATC1 translocation to the nucleus, where it interacts with a variety of transcription factors to control expression of target genes [Rao *et al.* 1997]. Since proper shuttling between cytoplasm and nucleus is essential for correct function of NFATC proteins, we first explored the impact of the three identified variants on NFATC1 subcellular localization. To this goal, immunofluorescence experiments were performed using COS-7 cells, which were transiently transfected to express either the wild-type or mutant EGFP-tagged NFATC1 proteins (Figure 2A). Following 48 hours incubation, the analysis revealed that the wild-type protein localizes in the nucleus in steady state conditions. Conversely, localization of two disease-associated mutants, p.(Val210Met) and p.(Ala696Thr) remained restricted to the cytoplasm; similarly, incomplete nuclear translocation was also observed for the p.(Ala367Val) mutant. To confirm the aberrant subcellular localization of disease-associated mutants, NFATC1 subcellular localization was assessed after stimulation with ionomycin, a drug known to increase intracellular levels of $Ca2^{+}$, and expected to efficiently activate calcineurin, and consequently promote more effectively nuclear translocation of NFATC1. After stimulation with ionomycin, a large fraction of the p.(Ala367Val) and p.(Ala696Thr) NFATC1 proteins was retained in the cytoplasm, further documenting impaired nuclear translocation. Such aberrant localization was particularly apparent in the mutant carrying the p.(Val210Met) change. To explore the hypothesis that the observed defective/impaired nuclear translocation of the three mutants resulted from structural

rearrangements affecting proper NLS recognition, subcellular localization of each mutant protein was assessed after transfecting cells with NFATC1 proteins containing an exogenous NLS at the N-terminus. Whereas the newly introduced NLS partially promoted nuclear import of the mutants, a large proportion of these proteins was still retained in the cytoplasm, confirming their variable impairment in the nuclear import.

To further validate this finding, immunoblot analysis of cytoplasmic and nuclear extracts was undertaken, before and after treatment with ionomycin. In both conditions, a nuclear-restricted localization was documented for wild-type NFATC1, while an aberrant distribution of mutants was observed. Consistent with the immunofluorescence analysis, the p.(Ala367Val) NFATC1 mutant was detected in both the cytoplasmic and nuclear fractions in untreated cells, while the other two mutants were present only in the cytoplasmic extract (Figure 2B). After treating cells for 30 minutes with 3μM ionomycin, a large amount of the mutant proteins was still visible in the cytoplasmic fraction, confirming the profound impact of mutations on NFATC1 subcellular localization.

To simulate the heterozygous expression of variants occurring in affected subjects, equal amounts of wild-type and mutant constructs were co-transfected to COS-7 cells and subcellular localization of NFATC1 was observed. Immunofluorescence studies showed that in cells coexpressing the wild-type protein concominantly with each of the p.(Ala367Val) or p.(Ala696Thr) mutants the *NFATC1* protein product was present in both the cytoplasm and nucleus whereas most of the protein was localized in the cytoplasm in cells co-transfected with the p.(Val210Met) mutant (Figure 2C). These data support a heterogeneous behavior of NFATC1 mutants with the p.(Val210Met) playing a dominant negative effect on wild-type NFATC1.

Impaired nuclear import of mutants would imply the presence of defective transcriptional control of target genes. To test this hypothesis the effect of each mutation on the transcriptional transactivation function of NFATC1 was analyzed by measuring the efficiency in activation of the *NPPB* promoter by luciferase assays. As shown in Figure 3, wild-type NFATC1 weakly activated the *NPPB* promoter basally, but more efficiently promoted the expression of the reported gene following treatment with 3 μM ionomycin. A similar extent of transactivation was obtained in the *NFATC1* construct containing an additional NLS. In contrast, all mutants showed a variably reduced activation of the *NPPB* promoter, in all conditions. Consistent with the immunofluorescence and cell fractioning data, such defective transactivation was particularly evident in the p.(Ala696Thr) and p.(Val210Met) NFATC1 mutants. To mimic the heterozygote condition, we co-transfected each mutant together with the wild-type and mesured the luciferase reporter activity. When equimolar amounts of wild-type and mutant DNA were transfected into COS7 cells, all examined mutations caused a significant reduction of normal NFATC1 activity, with p.(Val210Met) showing the most significant effect.

Together these results consistently suggest that AVSD-associated *NFATC1* mutants are inefficiently imported into the nucleus, have a significantly decreased transcriptional activity compared to the wild-type protein, and differentially impact on wild-type NFATC1 function.

In vivo functional impact of the AVSD-associated NFATC1 mutants

In vitro assessment of the AVSD-associated *NFATC1* mutants provided evidence for the significant impact of the three identified missense changes on protein function. To explore the clinical relevance of the variants, the consequences of ectopic expression of each of the three mutants on relevant developmental processes were analyzed *in vivo* using zebrafish as a

model system. Wild-type or mutant mRNA was microinjected in zebrafish embryos at one-cell stage. The resulting phenotypes were investigated at 24 and 48 hpf. As shown in Figure 4A, expression of p.(Val210Met), p.(Ala367Val) or p.(Ala696Thr) *NFATC1* mRNA resulted in heart edema and increased yolk extension, whereas expression of GFP alone or wild-type NFATC1 did not affect zebrafish development. No other obvious defects in other regions of embryos injected with mutant mRNAs were observed, indicating the cardiac-specific effects of the three *NFATC1* mutations. To further characterize the cardiac phenotype in response to expression of *NFATC1* variants, we examined the overall morphology and regionalization of the heart at 48 hpf by *in situ* hybridization, using a panel of cardiac markers, including *myl7* (heart tube), *amhc* (atrial myocardium), *vmhc* (ventricular myocardium) and *anf* (cardiac muscle cells). At this stage, the heart chambers are completely formed in wild-type embryos and the heart undergoes looping morphogenesis. As shown by *myl7* and *anf*–specific staining in embryos expressing mutant *NFATC1* mRNAs, the heart tube looping was either accelerated [p.(Val210Met) and p.(Ala367Val)]- or retarded p.(Ala696Thr) compared to controls. In contrast, myocardial chamber specification did not appear to be affected in mutant embryos, as determined by expression of *vmhc* and *amhc*. Next, we used a panel of atrioventricular canal (AVC) marker genes (*bmp4, tbx2b*, *NFAT* and *has2*) to evaluate the formation of the endocardial cushions, from which the atrioventricular valves develop. Compared to non-injected controls and wild-type *NFATC1*-expressing embryos, those expressing each of the three *NFATC1* mutants showed altered expression of AVC marker genes (Figure 4B), indicating altered AVC specification domains in these embryos. To better delineate the consequences of the *NFATC1* variants on AVC development, histological evaluation of the heart was performed. When compared to controls, all embryos injected with *NFATC1* mutant transcripts displayed an abnormal cardiac structure (Figure 4C), confirming

cardiac marker expression studies. Taken together, these data indicated that expression of AVSD-associated *NFATC1* alleles dramatically affected cardiac development by promoting abnormal heart looping and AVC development in a large proportion of embryos, without inducing gross defects in cardiac chamber specification.

DISCUSSION

Here, we report that heterozygous private/rare variants in *NFATC1* occur in a small proportion of isolated and syndromic AVSD cases. The identified missense changes result in a variably defective NFATC1 nuclear import and transcriptional function *in vitro*, and dramatically impact cardiac development *in vivo*, supporting their functional and clinical relevance. These results are in agreement with previous studies reporting the identification of *NFATC1* variants and CNVs encompassing the gene in patients with various congenital heart defects, including ventricular septal defects and tricuspid atresia [Abdul-Sater *et al*. 2012; Feng *et al*. 2016; Gu *et al*. 2011; Han *et al*. 2010; Khalil *et al*. 2017; Li *et al*. 2017; Shen *et al*. 2013; Wang *et al*. 2016; Yehya *et al.* 2006; Zhao *et al*. 2013]. These results are also in agreement with previous identification of AVSD-related variants in *CRELD1*, a gene acting as a regulator of calcineurin/NFATC1 signaling by promoting NFATC1 dephosphorylation and translocation to the nucleus. Identification of functional variants in both *NFATC1* and its upstream regulator *CRELD1* is consistent with a relevant role of the calcineurin/NFATC1 signaling in altering cardiac developmental programs implicated in AVSD onset. Of note, similar to *NFATC1* variants, which are present in both patients with isolated AVSD and with AVSD and HTX, heterozygous *CRELD1* variants were also identified in both isolated and syndromic AVSD forms [Guo *et al*. 2010; Maslen *et al*. 2006; Posch *et al*. 2008; Robinson *et*

al. 2003; Zatyka *et al*. 2005; Zhian *et al*. 2012]. These findings suggest that in some instances both isolated and syndromic forms of AVSD share a common genetic etiology, although further work on larger patient cohorts is needed for confirmation. Considering that human *CRELD1* mutations have also been identified as a risk genetic factor for AVSD in patients with DS, further studies are recommended to evaluate the presence and relevance of *NFATC1* mutations in DS patients with AVSD as well.

The NFAT signaling cascade is critical for diverse aspects of mammalian development and physiology, including processes controlling cardiac development [Crabtree and Olson, 2002; de la Pompa *et al.* 1998; Ranger *et al*. 1998]. An increase in intracellular Ca^{2+} concentration activates calcineurin, which dephosphorylates cytoplasmic NFAT proteins. Upon calcineurin-mediated dephosphorylation, nuclear localization signals are exposed and NFAT proteins translocate to the nucleus [Crabtree and Olson, 2002]. Once in the nucleus, NFAT proteins cooperate with each other or other transcription factors to regulate gene expression [Beals *et al*. 1997; Macian, 2005; Masuda et a. 1997; Okamura *et al*. 2000; Wu *et al*. 2013]. We performed functional analysis of the three missense variants to determine the extent to which these residue substitutions affect normal cell localization and transcriptional activity of the protein. Immunofluorescence and transactivation experiments revealed that localization of the p.(Val210Met) and p.(Ala696Thr) NFATC1 mutants remains restricted to the cytoplasm, and that these proteins display a significantly diminished transcriptional transactivation capacity. In contrast, the p.(Ala367Val) mutation was demonstrated to have milder impact on protein import to the nucleus. Consistent with the partially retained ability to translocate to the nucleus, this variant was shown to have a milder impact on the transcriptional function of NFATC1 compared to the other AVSD-related *NFATC1* changes. Both p.(Val210Met) and p.(Ala696Thr) more dramatically affected NFATC1 transactivation activity. Such effect

appeared to be enhanced when they were forced to enter the nuclei with ionomycin treatment or adding to the protein an exogenous NLS. Of note, p.(Val210Met) was demonstrated to drive a dominant negative behavior by imparing proper function of the wild-type protein by affecting its nuclear translocation upon stimulation. Further studies are required to understand whether the other two mutations have a qualitatively similar but milder dominant negative effect or result in a hypomorphic/inactive NFATC1 protein.

Whereas the p.(Ala367Val) variant was found in a patient with isolated AVSD, p.(Val210Met) and p.(Ala696Thr) were identified in syndromic patients with AVSD in the context of HTX with polysplenia. HTX is the most frequent extracardiac finding associated with AVSDs after trisomy 21 [Digilio *et al.* 1999], and refers to a combination of abnormal arrangement of the abdominal and thoracic organs with complex CHDs including AVSD, common atrium, anomalous systemic and pulmonary venous drainage, persistent left superior vena cava with unroofed coronary sinus, and conotruncal defects. HTX is genetically heterogeneous and it has been associated to mutations in at least 20 genes involved in establishing left-right asymmetry, such as those encoding for transducers participating to NODAL signaling or those causing primary ciliary dyskinesia (PCD). In principle, mutation in these genes could plausibly be causal for both the cardiac and extra-cardiac phenotypic characteristics of the *NFATC1*-mutated patients. However, screening of a panel of disease genes implicated in AVSD, HTX and OAVS was performed in the three NFATC1 mutation-positive cases, and none had genetic variations in major genes related to HTX, or showed the chronic respiratory tract infections typical of PCD, making unlikely this hypothesis. Nevertheles, given the complex and genetically heterogeneous architecture of AVSD, we cannot exclude that the identified *NFATC1* variations and other undisclosed loci may jointly contribute to predisposition to AVSD in our cases. Interestingly, the variant exhibiting the

milder phenotype, p.(Ala367Val) and partial maintainance of ability to translocate to the nucleus together with the highest transactivation activity among mutants, was found in a patient with isolated AVSD, while the other mutations, p.(Val210Met) and p.(Ala696Thr), which dramatically impacted the nuclear import and transactivation activity of the protein, were detected in patients with AVSD and HTX. These data suggest that different phenotypes might be associated to *NFATC1* mutations, and such clinical heterogeneity might be the result of a quantitatively or qualitatively differential impact of mutations on NFATC1 function. We hypothesize that different thresholds of NFATC1 function might be required in various developmental programs, which would explain the differential involvement of the extracardiac manifestations, like HTX and/or the OAVS phenotype, specifically associated with mutations with more severe impact on NFATC1 function. Of note, similarly to the *NFATC1* mutations reported here, a selected group of mutations in cilia genes, with roles in both hedgehog signaling and laterality, can cause distinct presentations of AVSDs and HTX both in mice and humans, with the more severe mutations causing both AVSDs and situs abnormalities and the milder ones resulting in AVSDs in the absence of situs abnormalities [Burnicka-Turek *et al.* 2016].

During early embryogenesis, left-right asymmetry of the body-axis is established via intricate cross-talk among multiple signaling pathways, such as notch, nodal, hedgehog, FGF and BMP, ultimately restricting NODAL signaling to the left side of the embryo [Andersen *et al*. 2014]. *NODAL*, *LEFTY2*, *ACVR2B*, *GDF1*, *CFC1*, *CITED2* and *ZIC3* expression has been localized to the laterality signaling pathway, and human mutations in these genes show a wide range of heart defects, many of which clustering around laterality defects, such as HTX and faulty heart looping [Andersen *et al.* 2014; De Luca *et al*. 2010]. The association of *NFATC1* mutations with enhanced susceptibility to AVSDs and laterality defects may be

ascribed to a possible signaling intersection between the calcineurin-NFAT pathway and signaling pathways determining left-right asymmetry. Our *in vivo* studies showed that mutant zebrafish hearts are characterized by defective looping stage development and altered AVC patterning, indicating that the identified *NFATC1* mutations do result in cardiac laterality defects when expressed in this animal model.

In addition to HTX, one of the *NFATC1*-mutated patient also presented features of OAVS, a non-random association of microtia, hemifacial microsomia with mandibular hypoplasia, ocular epibulbar dermoid, and cervical vertebral malformations [Gorlin *et al.* 1963; Rollnick *et al*. 1987]. Of note, AVSD is one of the CHDs more frequently associated with extracardiac anomalies [Ferencz *et al*. 1997], and CHDs have been reported in 5-58% of the OAVS patients, with AVSD in 2% of the cases [Calzolari *et al*. 2003; Digilio *et al*. 2008]. Subjects with OAVS-HTX complex have recurrently been described, suggesting the possibility that OAVS in these patients represent a component of a malformation complex involving the organization of asymmetric structures [Caramia et a. 1970; Lin *et al*. 1998; Maat-Kievit *et al*. 1994; Volpe and Gentile, 2004]. Interestingly, further testing of the patient using a multi-gene NGS panel including candidate genes for AVSD, HTX and OAVS identified an additional missense variant in *TBX1* gene, p.(Pro86Leu). *TBX1* encodes for a transcription factor of the T-box family, which plays important roles in the formation of tissues and organs during embryonic development. The gene maps to human chromosome 22q11.2, and changes in this gene, due to either a point mutation or a deletion of part of chromosome 22 encompassing *TBX1*, are considered to be responsible for many of the features of DiGeorge syndrome (DGS)/velocardiofacial syndrome (VCFS), a common congenital disorder characterized by neural-crest-related developmental defects. In the literature, 22q11.2 deletions have been also found to recur in patients with typical DGS/VCFS clinical features in association with

hemifacial microsomia and microtia [Digilio *et al*. 2009; Dos Santos *et al*. 2014; Lafay-Cousin *et al*. 2009; Spineli-Silva *et al*. 2017; Torti *et al*. 2013; Xu *et al.* 2008], suggesting possible OAVS candidate genes in this segment. In wiew of these findings, *TBX1* variant p.(Pro86Leu) likely represents the major determinant of the OAVS phenotype in the present patient, and the gene within 22q11.2 chromosome responsible for the OAVS features observed in patients with 22q11.2 deletion.

The collected data point to a relationship between defective NFATC1 function and AVSD. Like most of CHDs, the presently identified *NFATC1* mutated cases are sporadic. Beyond the 20% of sporadic CHD caused by *de novo* CNVs and SNVs, it is very likely that most CHDs are secondary to complex inheritance [Blue *et al.* 2017]. Therefore, we cannot exclude that other genetic variants, including either common SNPs or rare/private mutants, are contributing to CHD found in these patients.

In summary, we identified three rare, nonsynonymous *NFATC1* variants in patients with AVSD that significantly affect proper intracellular localization of the protein and its transcriptional activity, as well as the development of normal structure of the zebrafish heart. We also provided evidence for a dominant negative effect for one of the three variants. Taken together, these findings suggest that rare/private variants in *NFATC1* gene contribute to the genetic underpinnings of AVSD in humans with situs solitus and HTX.

ACKNOWLEDGEMENTS

The authors wish to thank the patients who participated in this research. Funding: This work was supported with grant support from the Italian Ministry of Health (RF 2010 2310935 and RC 2016 to A.D.L.), a grant from the Research Council for Earth and Life Sciences [ALW 819.02.021] with financial aid from the Netherlands Organisation for Scientific Research (NWO) (to J.d.H.), and Fondazione Bambino Gesù (CUoRE to M.T.).

DISCLOSURE STATEMENT

The authors declare that there is no conflict of interest regarding the publication of this article.

AUTHOR CONTRIBUTIONS

Conception and design: R.F., A.S., J.d.H., A.D.L.

Analysis and interpretation: R.F., V.G., A.S, T.M., M.C.D., M.T., B.M., J.d.H., A.D.L.

Data collection: R.F., M.B., F.C., V.G., F.L., P.V., S.G., G.C., K.M., F.P.S., H.H., M.C.D.,

Obtained funding: M.T., J.d.H., A.D.L.

Overall responsibility: M.T., B.M., J.d.H., A.D.L.

REFERENCES

Abdul-Sater Z, Yehya A, Beresian J, Salem E, Kamar A, Baydoun S, et al. 2012. Two heterozygous mutations in NFATC1 in a patient with Tricuspid Atresia. PLoS One 7:e49532.

Al Turki S, Manickaraj AK, Mercer CL, Gerety SS, Hitz MP, Lindsay S, et al. 2014. Rare variants in NR2F2 cause congenital heart defects in humans. Am J Hum Genet 94:574–585.

Amati F, Mari A, Digilio MC, Mingarelli R, Marino B, Giannotti A, et al. 1995. 22q11 deletions in isolated and syndromic patients with tetralogy of Fallot. Hum Genet 95:479–482.

Andersen TA, Troelsen Kde L, Larsen LA. 2014. Of mice and men: molecular genetics of congenital heart disease. Cell Mol Life Sci 71:1327–1352.

Asim A, Agarwal S, Panigrahi I, Sarangi AN, Muthuswamy S, Kapoor A. 2018. CRELD1 gene variants and atrioventricular septal defects in Down syndrome. Gene 641:180–185.

Beals CR, Sheridan CM, Turck CW, Gardner P, Crabtree GR. 1997. Nuclear export of NF-ATc enhanced by glycogen synthase kinase-3. Science 75:1930–1934.

Blue GM, Kirk EP, Giannoulatou E, Sholler GF, Dunwoodie SL, Harvey RP, Winlaw DS. 2017. Advances in the Genetics of Congenital Heart Disease: A Clinician's Guide. J Am Coll Cardiol 69:859–870.

Burnicka-Turek O, Steimle JD, Huang W, Felker L, Kamp A, Kweon J, et al. 2016. Cilia gene mutations cause atrioventricular septal defects by multiple mechanisms. Hum Mol Genet 25:3011–3028.

Calkoen EE, Hazekamp MG, Blom NA, Elders BB, Gittenberger-de Groot AC, Haak MC, Bartelings MM, Roest AA, Jongbloed MR. 2016. Atrioventricular septal defect: From embryonic development to long-term follow-up. Int J Cardiol 202:784–795.

Calzolari E, Garani G, Cocchi G, Magnani C, Rivieri F, Neville A, et al. 2003. Congenital heart defects: 15 years of experience of the Emilia-Romagna Registry (Italy). Eur J Epidemiol 18:773–780.

Caramia G, Di Battista C, Botticelli A. 1970. Goldenhar's syndrome. Description of a case with cardiovascular abnormalities, right lung agenesis and situs viscerum inversus. Minerva Pediatr 22:362–367.

Crabtree GR. 1999. Generic signals and specific outcomes: signaling through Ca2+, calcineurin, and NF-AT. Cell 96:611–614.

Crabtree GR, Olson EN. 2002. NFAT signaling: choreographing the social lives of cells. Cell 109 Suppl:S67–79.

D'Alessandro LC, Al Turki S, Manickaraj AK, Manase D, Mulder BJ, Bergin L, et al. 2016. Exome sequencing identifies rare variants in multiple genes in atrioventricular septal defect. Genet Med 18:189–198.

de la Pompa JL, Timmerman LA, Takimoto H, Yoshida H, Elia AJ, Samper E, et al. 1998. Role of the NF-ATc transcription factor in morphogenesis of cardiac valves and septum. Nature. 392:182–186.

De Luca A, Sarkozy A, Consoli F, Ferese R, Guida V, Dentici ML, et al. 2010. Familial transposition of the great arteries caused by multiple mutations in laterality genes. Heart 96:673–677.

Digilio MC, Marino B, Cicini MP, Giannotti A, Formigari R, Dallapiccola B. 1993. Risk of congenital heart defects in relatives of patients with atrioventricular canal. Am J Dis Child 147:1295–1297.

Digilio MC, Marino B, Toscano A, Giannotti A, Dallapiccola B. 1999. Atrioventricular canal defect without Down syndrome: a heterogeneous malformation. Am J Med Genet 85:140–146.

Digilio MC, Calzolari F, Capolino R, Toscano A, Sarkozy A, de Zorzi A, et al. 2008. Congenital heart defects in patients with oculo-auriculo-vertebral spectrum (Goldenhar syndrome). Am J Med Genet A 146A:1815–1819.

Digilio MC, McDonald-McGinn DM, Heike C, Catania C, Dallapiccola B, Marino B, Zackai EH. 2009. Three patients with oculo-auriculo-vertebral spectrum and microdeletion 22q11.2. Am J Med Genet A 149A:2860–2864.

Digilio MC, Pugnaloni F, De Luca A, Calcagni G, Baban A, Dentici ML, Versacci P, Dallapiccola B, Tartaglia M, Marino B. Atrioventricular canal defect and genetic syndromes: The unifying role of Sonic Hedgehog. Clin Genet. 2018 May 3. doi: 10.1111/cge.13375.

DiSegni E, Pierpont MEM, Bass JL, Kaplinsky E. 1985. Two dimensional echocardiography in detection of endocardial cushion defect in families. Am J Cardiol 55:1649–1652.

Dos Santos PA, de Oliveira SF, Freitas EL, Safatle HP, Rosenberg C, Ferrari I, Mazzeu JF. 2014. Non-overlapping 22q11.2 microdeletions in patients with oculo-auriculo-vertebral spectrum. Am J Med Genet A 164A:551–553.

Feng J, Hao J, Chen Y, Li F, Han J, Li R, et al. 2016. Chromosome microarray analysis of patients with 18q deletion syndrome. Zhonghua Yi Xue Yi Chuan Xue Za Zhi 33:203–207.

Ferencz C, Rubin JD, McCarter RJ, Brenner JI, Neill CA, Perry LW, et al. 1985. Congenital heart disease: prevalence at livebirth. The Baltimore-Washington Infant Study. Am J Epidemiol 121:31–36.

Ferencz C, Loffredo CA, Corea-Villasenor A, Wilson PD. 1997. Left-sided obstructive lesions. In Genetic and Environmental risks for major cardiovascular malformations: The Baltimore-Washington Infant Study 1981-1989. Baltimore Futura Publishing; pp 165–225.

García-Rodríguez C, Rao A. 1998. Nuclear factor of activated T cells (NFAT)-dependent transactivation regulated by the coactivators p300/CREB-binding protein (CBP). J Exp Med 187:2031–2036.

Garg V, Kathiriya IS, Barnes R, Schluterman MK, King IN, Butler CA, et al. 2003. GATA4 mutations cause human congenital heart defects and reveal an interaction with TBX5. Nature 424:443–447.

Giglio S, Graw SL, Gimelli G, Pirola B, Varone P, Voullaire L, et al. 2000. Deletion of a 5-cM region at chromosome 8p23 is associated with a spectrum of congenital heart defects. Circulation 102:432–437.

Gorlin RJ, Jue KL, Jacobsen U, Goldschmidt E. 1963. Oculoauriculovertebral dysplasia. J Pediatr 63:991–999.

Green EK, Priestley MD, Waters J, Maliszewska C, Latif F, Maher ER. 2000. Detailed mapping of a congenital heart disease gene in chromosome 3p25. J Med Genet 37:581–587.

Gu H, Gong J, Qiu W, Cao H, Xu J, Chen S, Chen Y. 2011. Association of a tandem repeat polymorphism in NFATc1 with increased risk of perimembranous ventricular septal defect in a Chinese population. Biochem Genet 49:592–600.

Guo Y, Shen J, Yuan L, Li F, Wang J, Sun K. 2010. Novel CRELD1 gene mutations in patients with atrioventricular septal defect. World J Pediatr 6:348–352.

Han ZQ, Chen Y, Tang CZ, Gao WG, Xie JY, Hu DY. 2010. Association between nuclear factor of activated T cells 1 gene mutation and simple congenital heart disease in children. Zhonghua Xin Xue Guan Bing Za Zhi 38:621–624.

Kircher M, Witten DM, Jain P, O'Roak BJ, Cooper GM, Shendure J. 2014. A general framework for estimating the relative pathogenicity of human genetic variants. Nat Genet. 46:310-315.

Lafay-Cousin L, Payne E, Strother D, Chernos J, Chan M, Bernier FP. 2009. Goldenhar phenotype in a child with distal 22q11.2 deletion and intracranial atypical teratoid rhabdoid tumor. Am J Med Genet A 149A:2855–2859.

Li CL, Niu L, Fu MY, Tian J, Wang QW, An XJ. 2017. Correlation between NFATC1 gene polymorphisms and congenital heart disease in children. Eur Rev Med Pharmacol Sci 21:3441–3446.

Lin HJ, Owens TR, Sinow RM, Fu PC Jr, DeVito A, Beall MH, et al. 1998. Anomalous inferior and superior venae cavae with oculoauriculovertebral defect: review of Goldenhar complex and malformations of left-right asymmetry. Am J Med Genet 75:88–94.

Maat-Kievit JA, Baraitser M, Winter RM. 1994. Total situs inversus associated with the oculo-auriculo-vertebral spectrum. Clin Dysmorphol 3:82–86.

Macian F. 2005. NFAT proteins: key regulators of T-cell development and function. Nat Rev Immunol 5:472–84.

Maslen CL, Babcock D, Robinson SW, Bean LJ, Dooley KJ, Willour VL, Sherman SL. 2006. CRELD1 mutations contribute to the occurrence of cardiac atrioventricular septal defects in Down syndrome. Am J Med Genet A 140:2501–2505.

Masuda ES, Liu J, Imamura R, Imai SI, Arai KI, Arai N. 1997. Control of NFATx1 nuclear translocation by a calcineurin-regulated inhibitory domain. Mol Cell Biol 17:2066–2075.

Meissner JD, Freund R, Krone D, Umeda PK, Chang KC, Gros G, Scheibe RJ. 2011. Extracellular signal-regulated kinase 1/2-mediated phosphorylation of p300 enhances myosin heavy chain I/beta gene expression via acetylation of nuclear factor of activated T cells c1. Nucleic Acids Res 39:5907–5925.

Molkentin JD, Lu JR, Antos CL, Markham B, Richardson J, et al. 1998. A calcineurin-dependent transcriptional pathway for cardiac hypertrophy. Cell 93:215–228.

Okamura H, Aramburu J, García-Rodríguez C, Viola JP, Raghavan A, Tahiliani M, et al. 2000. Concerted dephosphorylation of the transcription factor NFAT1 induces a conformational switch that regulates transcriptional activity. Mol Cell 6:539–550.

Posch MG, Perrot A, Schmitt K, Mittelhaus S, Esenwein EM, Stiller B, Geier C, Dietz R, Gessner R, Ozcelik C, Berger F. 2008. Mutations in GATA4, NKX2.5, CRELD1, and BMP4 are infrequently found in patients with congenital cardiac septal defects. Am J Med Genet A 146A:251–3.

Ranger AM, Grusby MJ, Hodge MR, Gravallese EM, de la Brousse FC, Hoey T, et al. 1998. The transcription factor NF-ATc is essential for cardiac valve formation. Nature. 1998;392:186–190.

Rao A, Luo C, Hogan PG. 1997. Transcription factors of the NFAT family: regulation and function. Annu Rev Immunol 15:707–447.

Reller MD, Strickland MJ, Riehle-Colarusso T, Mahle WT, Correa A. 2008. Prevalence of congenital heart defects in metropolitan Atlanta, 1998-2005. J Pediatr 153:807–813.

Robinson SW, Morris CD, Goldmuntz E, Reller MD, Jones MA, Steiner RD, et al. 2003. Missense mutations in CRELD1 are associated with cardiac atrioventricular septal defects. Am J Hum Genet 72:1047–1052.

Rollnick BR, Kaye CI, Nagatoshi K, Hauck W, Martin AO. 1987. Oculoauriculovertebral dysplasia and variants: phenotypic characteristics of 294 patients. Am J Med Genet 26:361–375.

Sarkozy A, Esposito G, Conti E, Digilio MC, Marino B, Calabrò R, Pizzuti A, Dallapiccola B. 2005. CRELD1 and GATA4 gene analysis in patients with nonsyndromic atrioventricular canal defects. Am J Med Genet A 139:236–238.

Sarkozy A, Lepri F, Marino B, Pizzuti A, Digilio MC, Dallapiccola B. 2006. Additional evidence that PTPN11 mutations play only a minor role in the pathogenesis of non-syndromic atrioventricular canal defect. Am J Med Genet A 140:1970–1972.

Sheffield VC, Pierpont ME, Nishimura D, Beck JS, Burns TL, Berg MA, et al. 1997. Identification of a complex congenital heart defect susceptibility locus by using DNA pooling and shared segment analysis. Hum Mol Genet 6:117–121.

Shen L, Li ZZ, Shen AD, Liu H, Bai S, Guo J, Yuan F, Li XF. 2013. Association of NFATc1 gene polymorphism with ventricular septal defect in the Chinese Han population. Chin Med J 126:78–81.

Smith KA, Joziasse IC, Chocron S, van Dinther M, Guryev V, Verhoeven MC. et al. 2009. Dominant-negative ALK2 allele associates with congenital heart defects. Circulation 119:3062–3069.

Spineli-Silva S, Bispo LM, Gil-da-Silva-Lopes VL, Vieira TP. 2017. Distal deletion at 22q11.2 as differential diagnosis in Craniofacial Microsomia: Case report and literature review. Eur J Med Genet 2017 Dec 27.

Thisse C, Thisse B, Schilling TF, Postlethwait JH. 1993. Structure of the zebrafish snail1 gene and its expression in wild-type, spadetail and no tail mutant embryos. Development 119:1203–1215.

Torti EE, Braddock SR, Bernreuter K, Batanian JR. 2013. Oculo-auriculo-vertebral spectrum, cat eye, and distal 22q11 microdeletion syndromes: a unique double rearrangement. Am J Med Genet A. 161A:1992–1998.

Volpe P, Gentile M. 2004. Three-dimensional diagnosis of Goldenhar syndrome. Ultrasound Obstet Gynecol 24:798–800.

Wang F, Wang H, Wang L, Zhou S, Chang M, Zhou J, Dou Y, Wang Y, Shi X. 2016. Association Between Single Nucleotide Polymorphisms in NFATC1 Signaling Pathway Genes and Susceptibility to Congenital Heart Disease in the Chinese Population. Pediatr Cardiol 37:1548–1561.

Westerfield. 1993. The ZebraWsh Book: a Guide for the Laboratory Use of ZebraWsh. The University of Oregon Press.

Wu B, Baldwin HS, Zhou B. 2013. Nfatc1 directs the endocardial progenitor cells to make heart valve primordium. Trends Cardiovasc Med 23:294–300.

Xu J, Fan YS, Siu VM. 2008. A child with features of Goldenhar syndrome and a novel 1.12 Mb deletion in 22q11.2 by cytogenetics and oligonucleotide array CGH: is this a candidate region for the syndrome? Am J Med Genet A 146A:1886–1889.

Yehya A, Souki R, Bitar F, Nemer G. 2006. Differential duplication of an intronic region in the NFATC1 gene in patients with congenital heart disease. Genome 49:1092–1098.

Zatyka M, Priestley M, Ladusans EJ, Fryer AE, Mason J, Latif F, Maher ER. 2005. Analysis of CRELD1 as a candidate 3p25 atrioventicular septal defect locus (AVSD2). Clin Genet 67:526–528.

Zhao W, Niu G, Shen B, Zheng Y, Gong F, Wang X, et al. 2013. High-resolution analysis of copy number variants in adults with simple-to-moderate congenital heart disease. Am J Med Genet A 161A:3087–3094.

Zhian S, Belmont J, Maslen CL. 2012. Specific association of missense mutations in CRELD1 with cardiac atrioventricular septal defects in heterotaxy syndrome. Am J Med Genet A 158A:2047–2049.

FIGURE LEGEND

Figure 1. Non-synonymous sequence variants in the *NFATC1* gene and their associated clinical characteristics. A. DNA sequence chromatograms of *NFATC1* variants found in patients with AVSD. The arrow indicates the site of the variant nucleotide position. The wild-type and mutated sequences are shown below the electropherograms. B. Annotation data for the non-synonymous sequence variants detected in the *NFATC1* gene (RefSeq: NM_006162.4): functional impact predictions from bioinformatics tools and information on allele frequency in Italian controls and public databases. C. Clinical characteristics of mutation-positive patients.

A

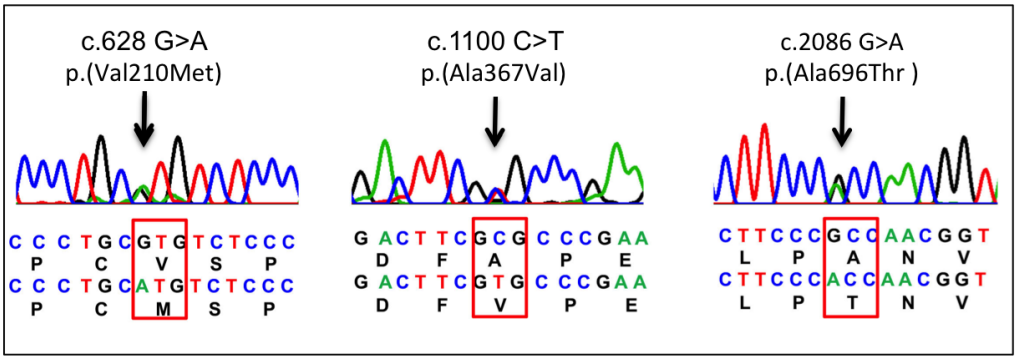

B

Subject	Nucleotide substitution	Ammino acid change	*CADD prediction	Control chromosomes	Allele Count	Human dbSNP variantion
HD239	c.628 G>A	p.(Val210Met)	28.8	0/1,600	A= 0.0011 (ESP6500) A= 0.000199681 (1000 Genomes) A= 0.0008 (ExAC)	rs62096875
CA12	c.1100 C>T	p.(Ala367Val)	9.984	0/1,600	T= 7.7E-5 (ESP6500) T= Absent (1000 Genomes) T= 2.9E-5 (ExAC)	rs367652299
IS18	c.2086 G>A	p.(Ala696Thr)	24.5	0/1,600	A= Absent (ESP6500) A= Absent (1000 Genomes) A= Absent (ExAC)	rs542259595

*CADD: a score greater or equal 10 indicates the 10% most deleterious substitutions of the human genome; a score greater or equal 20 indicates the 1% most deleterious. ESP6500: NHLBI ExomeSequencing Project; 1000 Genomes Project Phase 3 ExAC: Exome Aggregation Consortium.

C

Patient	Gender	Type of CHD	Other cardiac characteristics	Other clinical characteristics
HD239	Female	LAI, CA, Partial AVCD D ventricular loop Normaly related GA	Interruption IVC-AC	Polysplenia
CA12	Male	Situs solitus, Partial AVCD D ventricular loop Normaly related GA	None	None
IS18	Female	LAI, CA, Complete AVCD D ventricular loop Normally related GA	Dextrocardia, Interruption IVC-AC, PA, A-V block	Polysplenia, OAVS (HFM, preauricular tags, mild cognitive defect)

AVCD: Atrio Ventricular Canal Defect; LAI: Left Atrial Isomerism; CA: Common Atrium; GA: Great Arteries; HFM: Hemifacial Microsomia; IVC: Inferior Vena Cava; AC: Azygos Continuation; OAVS: oculo Auriculo Vertebral Spectrum; PA: Pulmonary atresia; A-V: Atrio-Ventricular.

Figure 2. Immunofluorescence localization and immunoblot analysis in COS-7 cells transfected with wild-type and mutant NFATC1 proteins [p.(Val210Met), p.(Ala367Val), and p.(Ala696Thr)]. A. Immunofluorescence analysis was performed on cells treated without or with ionomycin (3 mM, 30 minutes), and on cells transfected with NFATC1-NLS constructs. NFAT proteins (green), phalloidin marking actin filaments (red) and the nucleus (blue) were visualized. B. Immunoblot analysis of cytosolic and nuclear extracts before and after treatment with ionomycin. C. Immunofluorescence localization analysis in COS-7 cells co-transfected with wild-type and each of the mutant NFATC1 proteins.

A.

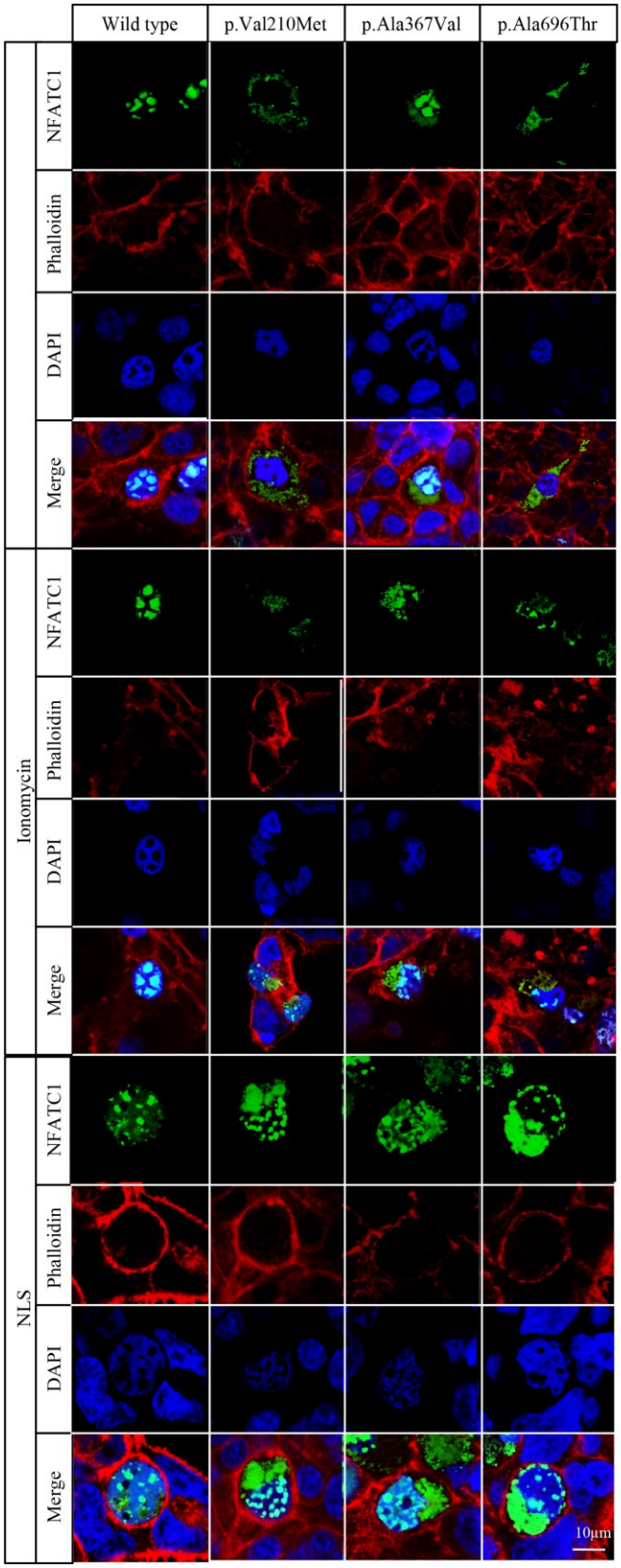

B

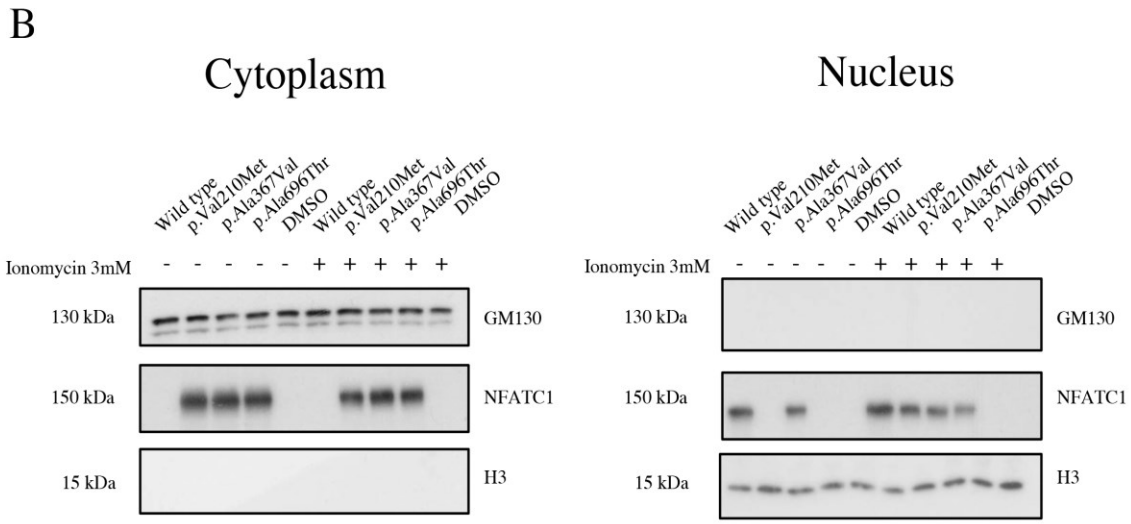

C

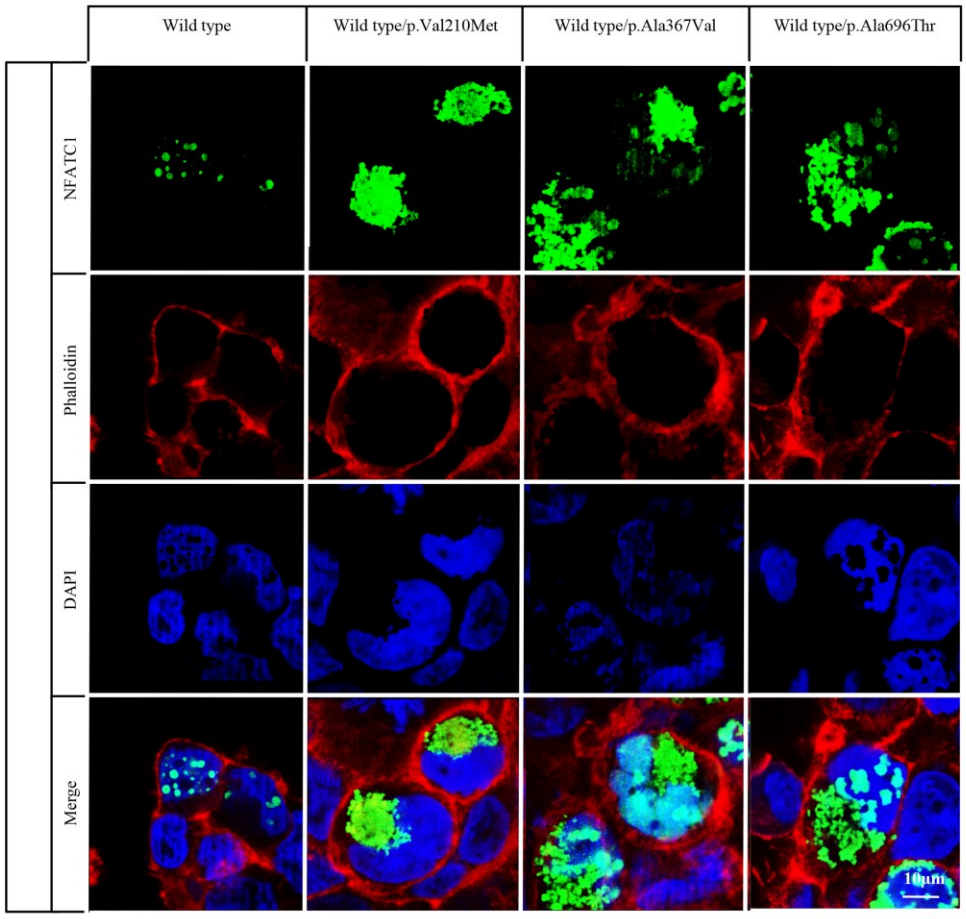

Figure 3. Dual luciferase assays (expressed as fold activation of Firefly luciferase relative to Renilla luciferase) of COS-7 cells transfected with either wild-type or mutant NFATC1 proteins, in presence of the luciferase reporter constructs, basally (solid columns) and after treatment with ionomycin (dotted columns) or after adding to the protein an exogenous NLS (striped columns), or when wild-type protein was expressed in combination with each of the three mutants (checkered columns). Error bars for all data shown represent one standard deviation and statistical significance was established by Student's t-test. Transfection control is an empty vector control. *Indicates $P < 0.05$ by t-test.

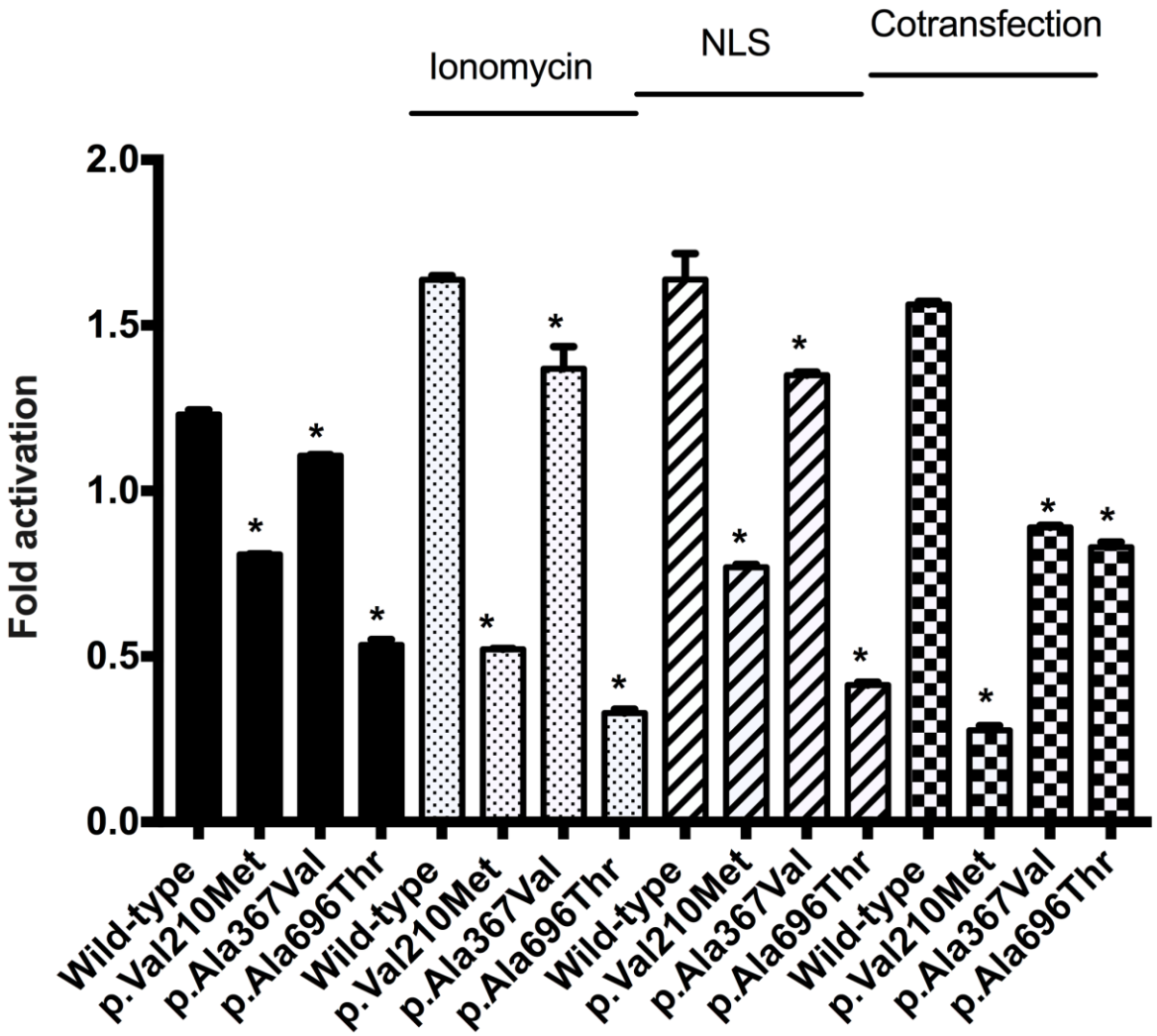

Figure 4. Zebrafish phenotype and heart characterization upon wild-type and mutant *NFATC1* RNA injection. A. Lateral views of *NFATC1*-injected embryos at 24 hpf (A, wild-type; B, p.(Val210Met); C, p.(Ala367Val); D, p.(Ala696Thr), and 48 hpf (A`, wild-type, B`, p.(Val210Met); C`, p.(Ala367Val); D`, p.(Ala696Thr). Arrows indicate heart edemas and yolk sac extension sites. B. Ventral views of 48 hpf embryos after *in situ* hybridization showing the expression of *myl7*, *amhc*, *vmhc*, *anf*, *bmp4*, *tbx2b*, *nfat*, *has2* in wild-type and *NFATC1* mutant embryos, and the number of embryos analyzed. C. Hematoxylin and eosin staining of transverse section of wild-type and mutant zebrafish. Numbers at the bottom right corner indicate the number of embryos displaying the illustrated phenotype vs. the total number of embryos examined.

A

B

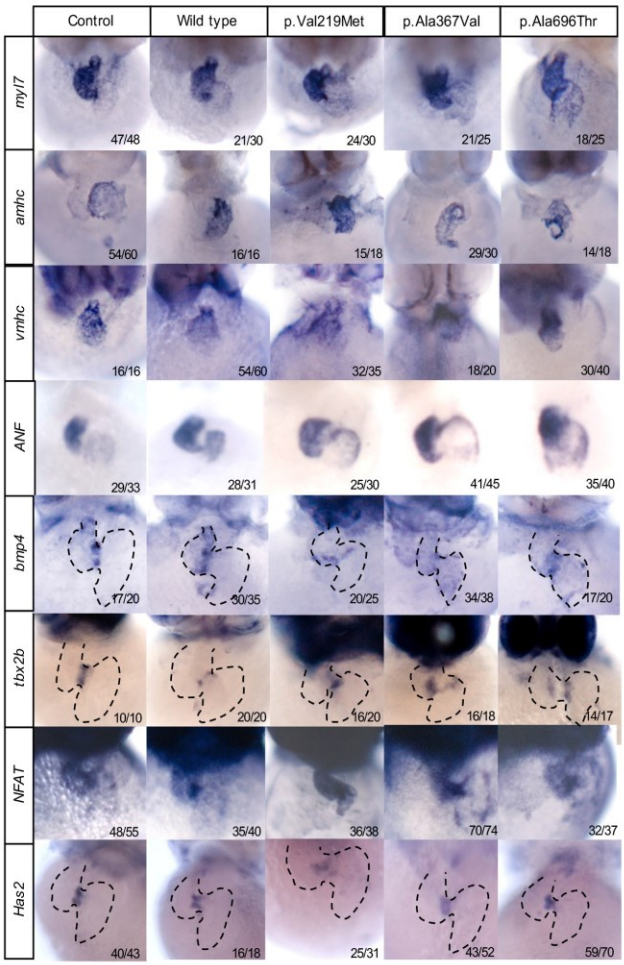

C

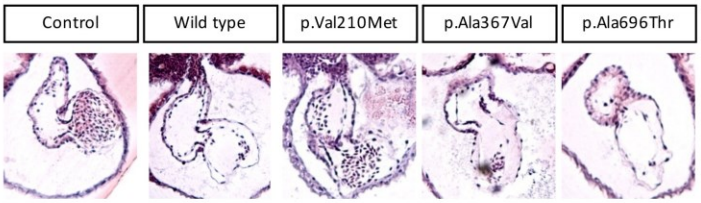

Supp. Figure S1. Alignment of amino acid residues adjacent to *NFATC1* p.(Val210Met), p.(Ala367Val) and p.(Ala696Thr) sequence variants showing level of conservation among different species. The amino acidic residue altered by the mutation is indicated by bold font (*Homo sapiens*, NP_001265598.1; *Pan troglodytes*, XP_512184.4; *Macaca mulatta*, XP_001088054.1; *Canis lupus familiaris*, XP_005615343.1; *Bos taurus*, NP_001160087.1; *Mus musculus*; NP_001157584.1, *Rattus norvegicus*, NP_001231862.1; *Gallus gallus*, XP_418906.4; *Danio rerio*, NP_001038624.1; *Xenopus Tropicalis*, NP_001072740.1.